

## Excitation functions for the production of $^{18}\text{F}$ and $^{24}\text{Na}$ from Al and Si with fast pions

B. J. Dropesky, G. W. Butler, G. C. Giesler, C. J. Orth, and R. A. Williams

*Isotope and Nuclear Chemistry Division, Los Alamos National Laboratory, Los Alamos, New Mexico 87545*

(Received 14 February 1985; revised manuscript received 24 June 1985)

The excitation functions for the pion-induced reactions  $^{27}\text{Al}(\pi^\pm, x\text{N})^{18}\text{F}$ ,  $^{27}\text{Al}(\pi^\pm, x\text{N})^{24}\text{Na}$ ,  $\text{Si}(\pi^\pm, x\text{N})^{18}\text{F}$ , and  $\text{Si}(\pi^\pm, x\text{N})^{24}\text{Na}$  have been determined for 50- to 390-MeV  $\pi^+$  and 50- to 500-MeV  $\pi^-$ . These excitation functions will enable experimenters to monitor high-intensity pion beams by activation of readily available high-purity Al foils or Si disks. The four excitation functions for  $^{18}\text{F}$  production and the two for  $^{24}\text{Na}$  production by  $\pi^+$  show similar (3,3) resonance patterns. However, those for  $^{24}\text{Na}$  production by  $\pi^-$  are strikingly different in that the cross sections remain large from the resonance energy on down. This feature is attributed to increasing contributions from  $\pi^-$  absorption and charge exchange with decreasing energy.

### I. INTRODUCTION

The advent of the "meson factories" and their relatively intense pion beams made it necessary to develop activation techniques to measure the pion fluxes, because it would no longer be possible to count individual particles by electronic means (at fluxes of  $10^8$  to  $10^9$   $\pi/\text{s}$ ), and the use of current integrating devices would be impractical for activation studies. This need was partially met by our measurement of the excitation functions of the  $^{12}\text{C}(\pi^\pm, \pi\text{N})^{11}\text{C}$  reactions over the energy ranges of 40–600 MeV for  $\pi^-$  and 50–520 MeV for  $\pi^+$  at the Clinton P. Anderson Meson Physics Facility (LAMPF) (Ref. 1) and over the range of 30–100 MeV for  $\pi^\pm$  at TRIUMF.<sup>2</sup> The absolute cross sections of these reactions were determined at pion particle rates low enough for electronic counting but sufficiently high to enable the 20.4-min  $^{11}\text{C}$  activity induced in carbon targets to be determined accurately. These carbon excitation functions serve as our primary pion beam monitors.

For a wide variety of pion-nucleus activation studies that require target irradiations longer than about 1 h, it is important to establish excitation functions of more practical secondary monitor reactions yielding longer-lived products. The reactions selected for this purpose, and measured relative to the above primary reactions, involve the production of 110-min  $^{18}\text{F}$  and 15-h  $^{24}\text{Na}$  in aluminum and silicon disks with both  $\pi^+$  and  $\pi^-$ . These products can be measured with good accuracy without requiring chemical separation. Also, because their formation involves more complex reactions than single nucleon removal, their cross sections were expected to vary more slowly across the (3,3) resonance than was observed for the  $^{12}\text{C}(\pi^\pm, \pi\text{N})^{11}\text{C}$  reactions.<sup>1</sup> The Al was chosen because thin, high purity uniform foils of the metal are readily available. However, because of the known low-energy threshold ( $\sim 6$  MeV) for the  $^{27}\text{Al}(n, \alpha)^{24}\text{Na}$  reaction that would be brought about by secondary neutrons in pion irradiations that require thick targets, silicon was also included in our study in order to provide a monitor that is

less sensitive to secondary neutrons. The threshold for the  $^{28}\text{Si}(n, \alpha\text{p})^{24}\text{Na}$  reaction is 15.2 MeV; for the low abundance  $^{29}\text{Si}$  and  $^{30}\text{Si}$  isotopes, the threshold for  $^{24}\text{Na}$  production by neutrons is higher.

Prior measurements of the pion cross sections reported in this study are meager. Reeder and Markowitz<sup>3</sup> measured the cross section for the production of  $^{24}\text{Na}$  from  $^{27}\text{Al}$  with  $\pi^-$  at several energies from 127 to 423 MeV. In a series of measurements of the cross section of the  $^{27}\text{Al}(\pi^-, x\text{N})^{18}\text{F}$  reaction from 450 to 1760 MeV, Poskanzer and Remsberg<sup>4</sup> provided one value to be compared with the present work. Comparisons with these measurements are made in Sec. IV A.

The measurement of these Al and Si reaction cross sections relative to the  $^{12}\text{C}(\pi^\pm, \pi\text{N})^{11}\text{C}$  reactions, over the energy ranges available for pion activation studies at LAMPF, was the primary goal of the present investigation. The procedure followed here is very similar to that carried out years ago to use activation techniques to monitor proton beams,<sup>5</sup> namely the establishment of the  $^{12}\text{C}(p, \text{pn})^{11}\text{C}$  excitation function by means of direct proton-counting techniques and subsequent measurement of the  $^{27}\text{Al}(p, 3\text{pn})^{24}\text{Na}$  excitation function relative to the former.

The study of the  $^{27}\text{Al}(\pi^\pm, x\text{N})^{18}\text{F}$ ,  $^{24}\text{Na}$  and  $\text{Si}(\pi^\pm, x\text{N})^{18}\text{F}$ ,  $^{24}\text{Na}$  cross sections over the region of the (3,3) pion-nucleon resonance had a second and equally important goal, that is, to provide insight into the mechanism of these pion-nucleus reactions involving the emission of from 3 to 12 nucleons.

### II. EXPERIMENTAL

#### A. Pion channels and beam tuning

The pion beams used for this study were obtained from two different channels at LAMPF: LEP (low energy pion channel) and P<sup>3</sup> (particle and pion physics channel). These channels are described in detail in Refs. 6 and 7, respectively. The range of energies selected on the LEP

channel was from 50 to 100 MeV. On the  $P^3$  channel,  $\pi^-$  energies from 70 to 500 MeV and  $\pi^+$  energies from 50 to 390 MeV were used. Both channels were tuned to produce a "waist" in the beam at the target position so that at least 99% of the beam was within the 3.8-cm diameter of the target disks. The beam spot varied somewhat in shape but would usually be included with a 2.5-cm diam circle. The momentum spread ( $\Delta P/P$ ) of the pion beam transmitted by each channel was normally adjusted to relatively large values (4–8%) in order to provide high beam intensity. Removal of protons from the high-energy  $\pi^+$  beams at the  $P^3$  channel was accomplished by differential energy degradation of the particles. From our previous work,<sup>1</sup> it was learned that proton contamination of the  $\pi^+$  beam could be reduced to a negligible amount up to about 400 MeV. Thus, our  $\pi^+$  measurements do not extend beyond this energy. The final step before irradiating a target packet was to expose a Polaroid film (high speed type 47) to the beam to determine the exact position of the beam spot for aligning the target.

### B. Targets and irradiations

The targets for this study consisted of packets of 3.8-cm diam circular disks of Pilot B plastic scintillator<sup>8</sup> (0.08, 0.16, or 0.32 cm thick), of aluminum (0.025, 0.05, 0.064, or 0.32 cm thick), and of elemental silicon (0.05 or 0.10 cm thick) or quartz ( $\text{SiO}_2$ , 0.1 cm thick). The target disks were consistently arranged in the above order and held together with small pieces of cellophane tape. During the irradiations, the Pilot B disk was always upstream of the others.

The Pilot B plastic contains 91.6% carbon by weight.<sup>8</sup> As in the previous work,<sup>1</sup> no correction was made for the 1.1%  $^{13}\text{C}$  content of the carbon; that is, the reference cross sections are based on the probability of production of  $^{11}\text{C}$  in natural carbon. Also, no correction was made for loss of  $^{11}\text{C}$  by diffusion from the irradiated plastic targets because this effect is negligible for such thick targets.<sup>9</sup>

A variety of aluminum disks were used in this study. For the earliest low-intensity runs, the 0.32-cm thick disks were punched from sheet stock that spectrographic analysis showed to be 98.5% Al, while the 0.064-cm thick disks were made from shim stock that analyzed at 98.6% Al. The impurities were such that their contributions to the yields of  $^{18}\text{F}$  and  $^{24}\text{Na}$  were negligible. All later runs at the higher fluxes were made with 0.025–0.05-cm thick disks of  $>99.9\%$  Al.

High purity silicon was used for all runs. A few early measurements on silicon were made with 0.1-cm thick disks of high purity quartz ( $>99.9\%$   $\text{SiO}_2$ ). All later measurements were made with precisely machined disks of detector-grade Si ( $>99.99\%$  Si); first, locally fabricated disks 0.1 cm thick and then commercially produced<sup>10</sup> 0.1- and 0.05-cm thick disks were used.

The target stacks were usually irradiated for a period of 40 min (two half-lives of  $^{11}\text{C}$ ). The pion intensities ranged from  $4 \times 10^5$  to  $5 \times 10^8$   $\pi/\text{s}$ .

### C. Activity measurements

After each irradiation, the target packet was disassembled, and each disk was counted on the appropriate counter(s). Three different counting systems were used: (1) a  $\beta$ - $\gamma$  coincidence system (described in Ref. 1) for measuring the absolute disintegration rate of the  $^{11}\text{C}$  activity induced in the Pilot B disks; (2) two NaI(Tl)  $\gamma$ - $\gamma$  coincidence systems for measuring the  $^{18}\text{F}$  positron activity (via the 511-keV annihilation quanta) in the Al and Si disks; and (3) two or three NaI(Tl)  $\gamma$  spectrometers for measuring the  $^{24}\text{Na}$  activity (via the 1369- and 2754-keV gamma rays).

The  $^{11}\text{C}$  positrons were self-detected by optically coupling the plastic target scintillator to the photomultiplier of the  $\beta$ - $\gamma$  coincidence system; the annihilation quanta were detected in the adjacent NaI(Tl) detector, which had an electronic window set to include only 511-keV photopeak pulses (window width: three times FWHM of photopeak). Each sample was counted for at least three half-lives, and the  $^{11}\text{C}$  disintegration rate was calculated from the net  $\beta^+$ ,  $\gamma$ , and  $\beta^+$ - $\gamma$  coincidence rates.<sup>11</sup> The data were fitted to a one-component exponential with a 20.4-min half-life by least-squares fitting.<sup>12</sup> No significant deviations were observed from the 20.4-min half-life.

The  $\gamma$ - $\gamma$  coincidence systems consisted of two 7.6-cm diam by 7.6-cm long NaI(Tl) detectors facing each other with the target disk between them, sandwiched between two 0.16-cm thick copper plates to ensure that all annihilation quanta originated in or near the target disk. An electronic window having a width three times the FWHM of the 511-keV annihilation photopeak was set for each detector. The efficiencies of these counting systems were frequency calibrated for annihilation radiation counting by measuring the  $^{11}\text{C}$   $\beta^+$  counting rate in some of the Pilot B disks prior to determining the absolute disintegration rate in the  $\beta$ - $\gamma$  counter. Counting of the Al and Si disks for  $^{18}\text{F}$  activity was started an hour or so after the end of the irradiation so that most of the small amount of 10-min  $^{13}\text{N}$  and 20.4-min  $^{11}\text{C}$  activities had decayed away. The counting usually continued for several half-lives of  $^{18}\text{F}$ . The contribution to the positron counting rate from the  $^{24}\text{Na}$  activity was always less than 1% of the initial  $^{18}\text{F}$  counting rate.

The  $^{24}\text{Na}$  activity produced in the Al and Si disks was measured after the  $^{18}\text{F}$  counting was completed. The samples were taped on the Al counting plate (0.15 cm thick) and counted face up directly above the NaI(Tl) detector. All pulses corresponding to an energy band ranging from just below the 1369-keV photopeak to just above the 2754-keV photopeak of  $^{24}\text{Na}$  were recorded as a function of time. The efficiencies of the several spectrometer systems used were established by counting special samples of  $^{24}\text{Na}$  prepared by transferring a measured aliquot of a standardized solution of the activity to an Al counting plate. The solution was transferred as small droplets over an area approximating the typical pion beam spot size; the droplets were evaporated to dryness, covered with cellophane tape, and counted. The  $^{24}\text{Na}$  solution was prepared by irradiating a few mg of high-purity  $\text{Na}_2\text{CO}_3$  in the thermal neutron flux of the Omega West Reactor and then dissolving in water to a known volume. A measured

TABLE I. Measured cross sections for the reactions  $^{27}\text{Al}, \text{Si}(\pi^+, x\text{N})^{18}\text{F}, ^{24}\text{Na}$ .

$T_{\pi^+}$ (MeV)	Monitor (mb) <sup>a</sup>	Aluminum		Silicon	
		$^{18}\text{F}$ (mb) <sup>b</sup>	$^{24}\text{Na}$ (mb)	$^{18}\text{F}$ (mb) <sup>b</sup>	$^{24}\text{Na}$ (mb)
50± 1	10.3±0.6	7.2±0.4(5) <sup>c</sup>	5.7±0.3(4)	6.3±0.5(5)	2.6±0.2(4)
60± 1	14.6±0.8	8.6±0.5(2)	6.0±0.4(2)	7.9±0.6(1)	3.0±0.3(1)
79± 2	25.2±1.3	10.7±0.4(3)	8.4±0.7(3)	9.8±0.4(3)	3.6±0.2(3)
99± 5	33.5±1.7	12.7±0.8(7)	12.7±0.7(6)	11.9±0.7(4)	4.6±0.2(3)
129± 2	42.0±2.1	13.9±0.5(2)	17.2±1.0(2)	13.0±0.5(2)	6.0±0.4(2)
149± 6	44.6±2.2	13.2±0.4(3)	18.8±0.8(3)	13.4±0.6(2)	7.0±0.4(3)
164±10	45.1±1.6	13.7±0.6(1)	19.5±0.7(1)	13.4±0.6(1)	7.2±0.3(1)
180± 5	44.0±1.5	13.8±0.5(1)	20.0±0.7(1)	13.5±0.5(1)	7.7±0.3(1)
197± 8	40.9±1.4	12.6±0.5(2)	19.6±1.0(2)	13.5±0.5(1)	7.6±0.4(2)
245± 8	30.8±1.1	10.7±0.3(3)	17.6±0.7(3)	10.7±0.3(2)	7.3±0.5(3)
296± 9	23.7±0.9	8.8±0.3(4)	13.0±0.8(3)	9.3±0.8(2)	5.7±0.4(4)
342±16	20.9±0.8	8.9±0.5(2)	11.6±0.6(2)	8.6±0.5(1)	5.1±0.3(2)
389±19	20.7±0.8	8.0±0.4(4)	9.8±0.4(4)	8.6±0.3(2)	4.4±0.1(4)

<sup>a</sup>Cross sections for the primary monitor reaction  $^{12}\text{C}(\pi^+, \pi\text{N})^{11}\text{C}$  from Ref. 2 for  $T_{\pi}$  up to 164 MeV and from Ref. 1 for  $T_{\pi} > 164$  MeV.

<sup>b</sup>These cross sections are not corrected for the 3.1% electron capture branch, but are based on the assumption that  $^{18}\text{F}$  decays 100% by positron emission.

<sup>c</sup>Values in parentheses are the number of measurements averaged.

aliquot of the solution was transferred by evaporation to the center of an Al counting plate over a small area corresponding approximately to the size of the National Bureau of Standards mixed  $\gamma$ -ray calibration sources. This  $^{24}\text{Na}$  sample was then counted at a distance of 10 cm from a calibrated Ge(Li) gamma spectrometer in order to establish the specific  $^{24}\text{Na}$  disintegration rate of the solution.

All  $^{18}\text{F}$  and  $^{24}\text{Na}$  decay data were fitted with a least squares method<sup>12</sup> to half-lives of 109.8 min for  $^{18}\text{F}$  and 15.05 h for  $^{24}\text{Na}$ . In the case of the  $^{18}\text{F}$  data, two other components were included in the analysis: a 20.4-min component to resolve out the small contribution of  $^{11}\text{C}$  that might have been present and a 15-h component to resolve out the  $^{24}\text{Na}$  contribution. The  $^{24}\text{Na}$  decay data fitted a one-component analysis. In computing the disintegration rates of the three species<sup>13</sup> involved in this study, the very weak (0.24%) electron capture branch in the  $^{11}\text{C}$  decay was ignored, as was the 0.061%  $\beta^-$  branch to the 3.867-MeV level of  $^{24}\text{Mg}$  in the  $^{24}\text{Na}$  decay. Also, no correction was made for the 3.1% electron capture branch in the decay of  $^{18}\text{F}$ ; therefore, the quoted cross sections are exclusively for the  $\beta^+$  activity induced in the target.

### III. RESULTS

The results of this study are presented in Tables I ( $\pi^+$ ) and II ( $\pi^-$ ) which list, as a function of pion energy, the reference values of cross sections of the primary monitor reactions,  $^{12}\text{C}(\pi^\pm, \pi\text{N})^{11}\text{C}$ , the measured cross sections for the production of  $^{18}\text{F}$  and  $^{24}\text{Na}$  from Al and Si targets, and the number of measurements averaged to give the determined cross section. Figures 1, 2, 3, and 4 show the excitation functions for the reactions  $^{27}\text{Al}(\pi^\pm, x\text{N})^{18}\text{F}, ^{24}\text{Na}$  and  $\text{Si}(\pi^\pm, x\text{N})^{18}\text{F}, ^{24}\text{Na}$ , respectively.

We have compiled in Tables III and IV sets of recom-

mended cross sections for these reactions. Smooth curves were drawn through the measured points in Figs. 1–4 to facilitate the extraction of cross sections at energies other than those measured. The uncertainties associated with the recommended values are derived from a simple averaging of uncertainties in the experimental points for each energy region.

The question of the contributions to the yields of  $^{18}\text{F}$  and  $^{24}\text{Na}$  from secondary reactions in our relatively thick targets was examined. Analysis of our measured yields from targets that varied in thickness from 578 to 1600 mg/cm<sup>2</sup> showed that within our uncertainties of measurement, no enhancement of the yields of these two species could be discerned for either  $\pi^+$  or  $\pi^-$  over the entire energy range studied. A special series of tests was carried out with target packets as thin as 143 mg/cm<sup>2</sup>, and the measured cross sections confirmed the earlier results that indicated that secondary reactions contributed less than 5% to the yields of  $^{18}\text{F}$  and  $^{24}\text{Na}$ .

## IV. DISCUSSION

### A. Comparisons with previous measurements

Only a few comparisons can be made with previous measurements on the reaction cross sections determined in this study. The values of Reeder and Markowitz<sup>3</sup> for the cross sections for the production of  $^{24}\text{Na}$  from  $^{27}\text{Al}$  with  $\pi^-$  at several energies are as follows: 13±3 mb at 127±9 MeV; 7±4 mb at 245±19 MeV; 9±2 mb at 373±10 MeV; and 5±1 mb at 423±10 MeV. These values are about half of what we observed, and no obvious explanation for the discrepancy is apparent. This is somewhat surprising in view of the fact that their cross sections for the  $^{12}\text{C}(\pi^-, \pi\text{N})^{11}\text{C}$  reaction over the energy range of 53 to 423 MeV, measured during the same study that included the measurements on aluminum, are in good agreement

TABLE II. Measured cross sections for the reactions  $^{27}\text{Al}, \text{Si}(\pi^-, x\text{N})^{18}\text{F}, ^{24}\text{Na}$ .

$T_{\pi^-}$ (MeV)	Monitor (mb) <sup>a</sup>	Aluminum		Silicon	
		$^{18}\text{F}$ (mb) <sup>b</sup>	$^{24}\text{Na}$ (mb)	$^{18}\text{F}$ (mb) <sup>b</sup>	$^{24}\text{Na}$ (mb)
50± 1	6.1±0.5	5.9±0.6(4) <sup>c</sup>	19.6±1.6(4)	6.6±0.8(4)	12.8±1.3(4)
60± 2	10.6±0.6	7.4±0.3(3)	20.2±1.8(4)	8.1±0.3(3)	12.8±0.6(2)
70± 2	16.4±0.8	8.1±0.3(1)	23.4±1.1(2)	8.2±0.6(2)	13.6±0.9(1)
80± 1	23.3±1.2	8.8±0.3(5)	22.5±0.9(5)	9.3±0.3(5)	13.4±0.4(5)
100± 2	37.2±2.0	9.8±0.6(7)	26.0±1.8(7)	10.1±0.7(6)	12.7±0.7(7)
110± 2	44.6±2.3	10.1±0.5(1)	25.4±1.3(1)	10.6±0.6(1)	12.8±0.5(2)
120± 8	51.5±2.6	10.8±0.4(2)	25.8±1.1(2)	11.2±0.4(2)	12.9±0.6(2)
150±11	65.6±3.3	11.8±0.4(2)	26.4±1.4(2)	12.1±0.6(2)	13.2±0.7(2)
160± 6	68.0±3.4	11.5±0.4(2)	25.0±0.9(2)	12.0±0.4(2)	12.4±0.4(3)
180±12	70.0±2.0	10.9±1.1(6)	23.8±0.5(6)	12.0±1.1(5)	12.0±0.3(5)
190±14	70.2±2.1	11.3±0.3(2)	24.3±1.6(1)	11.9±0.3(2)	12.3±0.8(1)
200±11	69.8±2.1	11.4±0.4(1)	22.9±0.7(1)	11.8±0.4(1)	11.3±0.4(1)
220± 3	66.6±2.0	10.8±0.3(1)	20.7±0.6(1)	10.6±0.3(1)	9.8±0.3(1)
250±17	58.3±1.8	9.5±0.4(2)	17.2±0.7(2)	9.7±0.3(2)	8.8±0.4(2)
300±16	44.7±1.4	9.0±0.2(3)	15.3±0.5(3)	9.7±0.2(3)	7.8±0.3(3)
350±24	34.4±1.1	7.7±0.3(1)	12.9±0.9(1)	8.5±0.3(1)	6.6±0.5(1)
400±25	27.3±0.9	7.2±0.2(2)	11.7±0.6(2)	7.9±0.2(2)	6.1±0.3(2)
450±22	23.4±0.8	6.7±0.2(2)	11.0±0.5(2)	7.6±0.2(2)	5.7±0.3(2)
500±24	21.0±0.7	6.6±0.2(2)	11.4±0.6(2)	7.6±0.4(2)	6.2±0.4(2)

<sup>a</sup>Cross sections for the primary monitor reaction  $^{12}\text{C}(\pi^-, \pi\text{N})^{11}\text{C}$  from Ref. 2 for  $T_{\pi}$  up to 164 MeV and from Ref. 1 for  $T_{\pi} > 164$  MeV.

<sup>b</sup>These cross sections are not corrected for the 3.1% electron capture branch, but are based on the assumption that  $^{18}\text{F}$  decays 100% by positron emission.

<sup>c</sup>Values in parentheses are the number of measurements averaged.

with ours.<sup>1</sup> Poskanzer and Remsberg<sup>4</sup> determined a value of  $6.2 \pm 0.8$  mb for the cross section for the  $^{27}\text{Al}(\pi^-, x\text{N})^{18}\text{F}$  reaction at 450 MeV, in agreement with our value of  $6.7 \pm 0.2$  mb at this energy.

From the work of Ashery *et al.*,<sup>14</sup> in which they determined the cross sections for reactions leading to various residual nuclear levels from  $\pi^+$  and  $\pi^-$  interactions in Al and Si by on-line prompt  $\gamma$ -ray measurements, we note that at 100 MeV only  $1.8 \pm 0.9$  mb goes into the  $^{27}\text{Al}(\pi^+, x\text{N})^{18}\text{F}$  reaction leading to the first excited state

of  $^{18}\text{F}$ . This is to be compared with our cross section of  $12.7 \pm 0.8$  mb for the reactions leading to all particle-bound states of  $^{18}\text{F}$ . In the more recent work of Lieb *et al.*,<sup>15</sup> in which on-line prompt  $\gamma$ -ray measurements again were used to determine the cross sections of a variety of  $\pi^+$  and  $\pi^-$  interactions in Al and Si, we are able to compare our results only with their  $^{18}\text{F}$  yields. For 190-MeV  $\pi^+$  reactions in  $^{27}\text{Al}$  and Si, their  $^{18}\text{F}$  cross sections are  $2.9 \pm 0.6$  and  $4.8 \pm 1.0$  mb, respectively (compared to our values of about 13 mb), and for 220-MeV  $\pi^-$  reac-

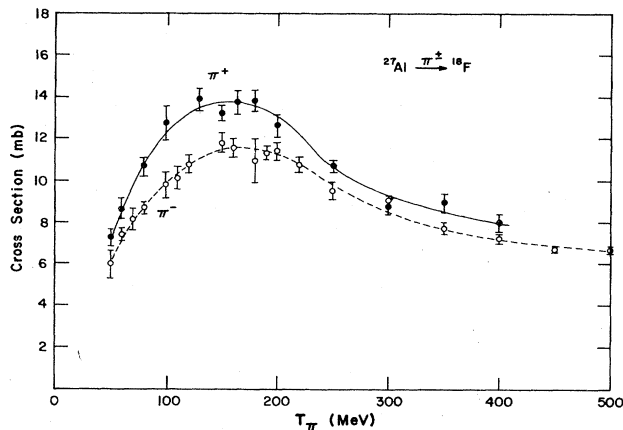


FIG. 1. Excitation functions for the reactions  $^{27}\text{Al}(\pi^{\pm}, x\text{N})^{18}\text{F}$ . The smooth curves are to guide the eye.

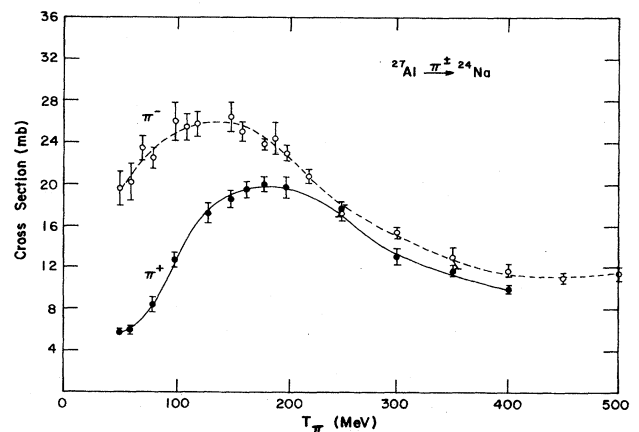
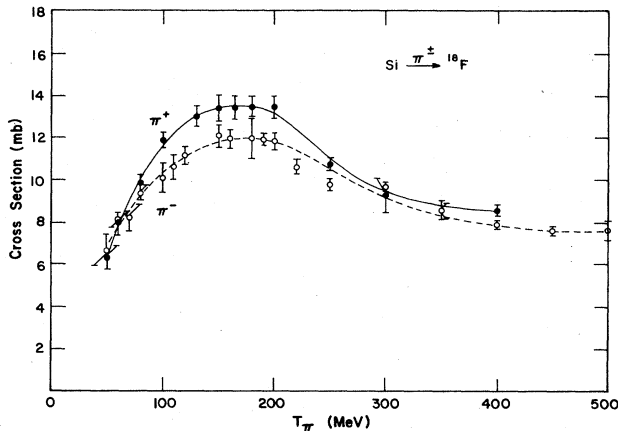
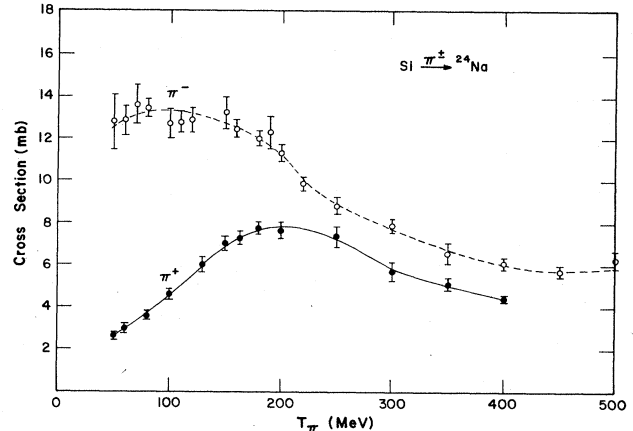


FIG. 2. Excitation functions for the reactions  $^{27}\text{Al}(\pi^{\pm}, x\text{N})^{24}\text{Na}$ .

FIG. 3. Excitation functions for the reactions  $\text{Si}(\pi^\pm, x\text{N})^{18}\text{F}$ .FIG. 4. Excitation functions for the reactions  $\text{Si}(\pi^\pm, x\text{N})^{24}\text{Na}$ .

tions on  $^{27}\text{Al}$  and  $\text{Si}$ , they are  $3.9 \pm 0.8$  and  $3.0 \pm 0.7$  mb, respectively (compared to ours of about 10.7 mb). Again, we see that the prompt  $\gamma$  technique provides only a fraction (about 30%) of the total reaction cross section we observe leading to all particle-bound states of  $^{18}\text{F}$ . Lieb *et al.* calculated a "compensated" cross section by using all available  $\gamma$ -ray feeding information and assuming a statistical  $2J + 1$  initial population of all states of  $^{18}\text{F}$ , but they succeeded in accounting for only 47–65% of the total production cross section observed in the present study.

### B. The excitation functions

Some of the more obvious features of the excitation functions determined in this study are the following. The

effect of the (3,3) pion-nucleon resonance in the region of 100 to 250 MeV is apparent, although its influence is considerably diminished for these more complex reactions in comparison to the  $^{12}\text{C}$  neutron knockout reactions.<sup>1,2</sup> Also, the effect of the charge of the pion on these cross sections is clear and consistent. Namely, when the addition of the positive charge of the  $\pi^+$  to the target nucleus results in the compound system being slightly to the neutron-deficient side of  $\beta$  stability (e.g.,  $^{27}\text{Al} + \pi^+ \rightarrow ^{27}\text{Si}$ ), the cross section for the production of the neutron-deficient species  $^{18}\text{F}$  is greater than when the addition of a negative pion charge results in a shift to the neutron-rich side of  $\beta$  stability. The converse is consistently true, as seen from the excitation functions for the production of the slightly neutron-rich species  $^{24}\text{Na}$ .

TABLE III. Recommended cross sections for the reactions  $^{27}\text{Al}, \text{Si}(\pi^\pm, x\text{N})^{18}\text{F}, ^{24}\text{Na}$ .

$T_{\pi^+}$ (MeV)	Aluminum		Silicon	
	$^{18}\text{F}$ (mb)	$^{24}\text{Na}$ (mb)	$^{18}\text{F}$ (mb)	$^{24}\text{Na}$ (mb)
50	7.2±0.4	4.9±0.3	6.3±0.5	2.6±0.2
60	8.3±0.4	6.0±0.4	7.7±0.5	2.9±0.2
70	9.5±0.5	7.4±0.5	9.0±0.5	3.3±0.2
80	10.7±0.6	9.0±0.6	10.1±0.5	3.7±0.2
90	11.7±0.6	11.0±0.7	11.0±0.5	4.1±0.2
100	12.7±0.6	12.8±0.8	11.7±0.5	4.5±0.2
110	13.1±0.6	14.5±0.8	12.2±0.5	5.0±0.2
120	13.5±0.6	15.9±0.9	12.7±0.6	5.4±0.3
130	13.7±0.6	17.0±0.9	13.0±0.6	5.9±0.3
140	13.8±0.5	18.0±0.9	13.2±0.6	6.4±0.3
150	13.9±0.5	18.7±0.9	13.3±0.6	6.8±0.4
160	13.9±0.5	19.2±0.9	13.4±0.6	7.2±0.4
170	13.8±0.5	19.6±0.8	13.4±0.5	7.4±0.3
180	13.6±0.5	19.8±0.8	13.3±0.5	7.6±0.3
190	13.3±0.5	19.9±0.8	13.2±0.5	7.7±0.4
200	12.7±0.4	19.8±0.8	12.9±0.5	7.8±0.4
250	10.4±0.4	17.7±0.8	10.7±0.5	7.3±0.5
300	9.4±0.4	13.3±0.7	9.3±0.5	5.8±0.4
350	8.7±0.4	11.2±0.6	8.8±0.5	5.0±0.3
400	8.1±0.4	9.8±0.5	8.5±0.4	4.4±0.2

TABLE IV. Recommended cross sections for the reactions  $^{27}\text{Al}, \text{Si}(\pi^-, x\text{N})^{18}\text{F}, ^{24}\text{Na}$ .

$T_{\pi^-}$ (MeV)	Aluminum		Silicon	
	$^{18}\text{F}$ (mb)	$^{24}\text{Na}$ (mb)	$^{18}\text{F}$ (mb)	$^{24}\text{Na}$ (mb)
50	6.0±0.4	19.6±1.7	6.8±0.5	12.5±0.9
60	7.1±0.4	21.2±1.5	7.8±0.6	12.9±0.9
70	8.0±0.4	22.5±1.3	8.7±0.5	13.1±0.8
80	8.7±0.4	23.5±1.2	9.3±0.5	13.3±0.7
90	9.4±0.4	24.3±1.2	10.0±0.5	13.4±0.6
100	9.9±0.5	24.9±1.3	10.5±0.4	13.4±0.6
110	10.4±0.5	25.4±1.4	10.9±0.4	13.3±0.6
120	10.8±0.4	25.8±1.3	11.2±0.4	13.2±0.6
130	11.1±0.4	26.0±1.2	11.5±0.4	13.0±0.6
140	11.4±0.4	26.0±1.2	11.7±0.5	12.9±0.6
150	11.5±0.4	26.0±1.1	11.8±0.5	12.7±0.6
160	11.5±0.5	25.7±1.0	11.9±0.5	12.5±0.5
170	11.5±0.5	25.3±1.0	12.0±0.5	12.3±0.5
180	11.4±0.6	24.7±1.0	11.9±0.5	12.0±0.5
190	11.3±0.5	24.0±1.0	11.8±0.4	11.6±0.5
200	11.2±0.4	23.0±1.0	11.6±0.3	11.3±0.5
250	9.8±0.3	17.3±0.8	10.1±0.3	8.9±0.4
300	8.6±0.3	14.5±0.7	9.1±0.3	7.8±0.4
350	7.8±0.2	12.9±0.7	8.4±0.3	6.7±0.4
400	7.2±0.2	11.8±0.7	7.9±0.3	6.0±0.4
450	6.9±0.2	11.2±0.6	7.7±0.3	5.7±0.3
500	6.5±0.2	10.8±0.5	7.6±0.3	5.8±0.3

These effects can be seen in Figs. 1–4. These observations are in accord with those reported<sup>16</sup> earlier from our study of the spallation of copper with fast pions of both charges.

The shapes and magnitudes of the four excitation functions for the production of  $^{18}\text{F}$  (Figs. 1 and 3) are very similar. This is not surprising, because they each represent the averaging of many reaction channels leading to this relatively deep spallation product, and there is only a 10% difference in  $\Delta A$  for producing  $^{18}\text{F}$  from  $^{27}\text{Al}$  and  $^{28}\text{Si}$  (92.2% abundant). On the other hand, the excitation functions for the production of  $^{24}\text{Na}$  (Figs. 2 and 4) exhibit striking differences between the  $\pi^+$ - and  $\pi^-$ -induced reactions below about 200 MeV. We note that for the  $\pi^+$ -induced reactions the cross sections at 50 MeV are about 26% and 38% of the values at 150 MeV for  $^{27}\text{Al}$  and Si, respectively, whereas for the  $\pi^-$ -induced reactions the cross sections decrease only to about 75% and 98% of their 150 MeV values at 50 MeV for Al and Si, respectively.

We also note that above about 150 MeV, the shapes of the excitation functions for  $^{24}\text{Na}$  production by  $\pi^-$  reactions in Al and Si are remarkably similar, but differ by a factor of 2 in magnitude. This may be accounted for simply by the fact that for  $^{24}\text{Na}$  production from  $^{28}\text{Si}$  the  $\Delta A=4$  or 33% more than the  $\Delta A=3$  for  $^{27}\text{Al}$ , and the  $\Delta A=5$  for  $^{29}\text{Si}$  (4.7%) and  $\Delta A=6$  for  $^{30}\text{Si}$  (3.1%) can only contribute toward decreasing the probability for  $^{24}\text{Na}$  production from Si relative to Al. The somewhat greater than a factor of 2 difference for the  $\pi^+$  production of  $^{24}\text{Na}$  from Al vs Si is probably related to the same arguments.

Qualitatively, these  $\pi^+$ - $\pi^-$  differences in the low energy cross sections for reactions leading to the small  $\Delta A$  product  $^{24}\text{Na}$  can be understood in terms of both absorption and single charge exchange processes. In the case of  $\pi^+$  absorption on an np or nn pair in  $^{27}\text{Al}$  followed by the emission of a pp or np pair, respectively, only the decay of the excited  $^{25}\text{Mg}^*$  nucleus by proton emission can lead to  $^{24}\text{Na}$ . However, for the  $\pi^-$  absorption on an np or pp pair leading to the emission of an nn or np pair, the decay of the residual nuclei  $^{25}\text{Mg}^*$  and  $^{25}\text{Na}^*$  by emission of a proton and neutron, respectively, both lead to  $^{24}\text{Na}$ . Similar processes can be traced through for the  $\pi^+$ - and  $\pi^-$ -induced reactions in the isotopes of silicon leading to the production of  $^{24}\text{Na}$ . Therefore, because pion absorption is known to become a larger fraction of the total reaction cross section with decreasing energy below the resonance region, the above difference favoring  $\pi^-$  over  $\pi^+$  production of  $^{24}\text{Na}$  would be expected to increase in going from 150 to 50 MeV.

Additionally, the single charge exchange reaction  $^{27}\text{Al}(\pi^+, \pi^0)^{27}\text{Si}^*$  must be followed by the energetically unfavorable emission of three protons from the excited  $^{27}\text{Si}^*$  to lead to  $^{24}\text{Na}$ . On the other hand, the reaction  $^{27}\text{Al}(\pi^-, \pi^0)^{27}\text{Mg}^*$  followed by the energetically more favorable emission of a triton or a proton and two neutrons leads to  $^{24}\text{Na}$ . In a study of single charge exchange reactions in  $^{27}\text{Al}$ ,  $^{45}\text{Sc}$ , and  $^{65}\text{Cu}$  leading to multiple bound states in the residual nucleus,<sup>17</sup> we observed a monotonic increase in the cross sections in going from 300 to about 100 MeV. Subsequent measurements of the  $^{27}\text{Al}(\pi^-, \pi^0)^{27}\text{Mg}$  reaction cross section showed it continuing to rise down to 50 MeV. From this evidence we con-

jecture that the inclusive cross section for single charge exchange reactions in complex nuclei rises monotonically from 150 to 50 MeV. Thus, the above difference favoring  $\pi^-$  over  $\pi^+$  production of  $^{24}\text{Na}$  via single charge exchange will also contribute to our observed low-energy cross sections on  $^{27}\text{Al}$ .

The almost constant cross section of about 12 mb from 50 to 150 MeV for the production of  $^{24}\text{Na}$  from Si may also be accounted for by an appreciable contribution due to single charge exchange. Considering only reactions in the 92% abundant  $^{28}\text{Si}$ , we see that the reaction  $^{28}\text{Si}(\pi^+, \pi^0)^{28}\text{P}^*$  must be followed by the energetically unfavored and highly improbable emission of four protons in order to lead to  $^{24}\text{Na}$ . In sharp contrast, the reaction  $^{28}\text{Si}(\pi^-, \pi^0)^{28}\text{Al}^*$  followed by the energetically favorable emission of an  $\alpha$  particle leads to  $^{24}\text{Na}$ . Thus, single charge exchange as well as absorption processes can reasonably account for the  $\pi^+ - \pi^-$  differences in the low energy portions of the measured excitation functions for production of the relatively near-target species  $^{24}\text{Na}$ .

In summary, we have established a set of excitation functions for the reactions  $^{27}\text{Al}(\pi^\pm, x\text{N})^{18}\text{F}, ^{24}\text{Na}$  and

$\text{Si}(\pi^\pm, x\text{N})^{18}\text{F}, ^{24}\text{Na}$ . A set of recommended cross sections as a function of pion kinetic energy is provided; these cross sections should prove very useful for monitoring the flux of intense pion beams by means of foil activation techniques. The persistence of relatively high values for the cross sections for the production of  $^{24}\text{Na}$  by  $\pi^-$  for energies below  $\sim 150$  MeV can be qualitatively understood in terms of specific pion absorption and single charge exchange processes.

#### ACKNOWLEDGMENTS

We gratefully acknowledge the work of the LAMPF technical staff and operating crews for enabling us to carry out these numerous target irradiations. Our gratitude is expressed to L. C. Liu and to A. L. Turkevich for many helpful discussions. We thank D.C. Hoffman and J. E. Sattizahn for their encouragement and support of this research. This work was performed under the auspices of the Division of Nuclear Physics of the U.S. Department of Energy.

<sup>1</sup>B. J. Dropesky, G. W. Butler, C. J. Orth, R. A. Williams, M. A. Yates-Williams, G. Friedlander, and S. B. Kaufman, Phys. Rev. C **20**, 1844 (1979).

<sup>2</sup>G. W. Butler, B. J. Dropesky, C. J. Orth, R. E. L. Green, R. G. Korteling, and G. K. Y. Lam, Phys. Rev. C **26**, 1737 (1982).

<sup>3</sup>P. L. Reeder and S. S. Markowitz, Phys. Rev. **133**, B639 (1964); P. L. Reeder, Lawrence Berkeley Laboratory Report UCRL-10531, 1962 (unpublished).

<sup>4</sup>A. M. Poskanzer and L. P. Rensberg, Phys. Rev. **134**, B779 (1964).

<sup>5</sup>J. B. Cumming, Annu. Rev. Nucl. Sci. **13**, 261 (1963).

<sup>6</sup>R. L. Burman, R. Fulton, and M. Jacobson, Nucl. Instrum. Methods **131**, 29 (1975).

<sup>7</sup>R. D. Werbeck and R. J. Macek, IEEE Trans. Nucl. Sci. **22**, 1958 (1975).

<sup>8</sup>Formerly produced by Pilot Chemicals Division, New England Nuclear Corp., Watertown, MA, but currently manufactured by Nuclear Enterprises, Inc., San Carlos, CA.

<sup>9</sup>J. B. Cumming, A. M. Poskanzer, and J. Hudis, Phys. Rev. Lett. **6**, 484 (1961).

<sup>10</sup>Monsanto Commercial Production, Inc., P. O. Box 8, St. Peters, MO 63376.

<sup>11</sup>L. P. Rensberg, Annu. Rev. Nucl. Sci. **17**, 347 (1967).

<sup>12</sup>J. B. Cumming, U. S. Atomic Energy Commission Report NAS-NS-3017, 1963 (unpublished), p. 25.

<sup>13</sup>Table of Isotopes, 7th ed., edited by C. M. Lederer and V. S. Shirley (Wiley, New York, 1978).

<sup>14</sup>D. Ashery, M. Zaider, Y. Shamai, S. Cochavi, M. A. Moines-ter, A. I. Yavin, and J. Alster, Phys. Rev. Lett. **32**, 943 (1974).

<sup>15</sup>B. J. Lieb, H. O. Funsten, C. E. Stronach, H. S. Plendl, and V. G. Lind, Phys. Rev. C **18**, 1368 (1978).

<sup>16</sup>C. J. Orth, B. J. Dropesky, R. A. Williams, G. C. Giesler, and J. Hudis, Phys. Rev. C **18**, 1426 (1978).

<sup>17</sup>R. S. Rundberg, B. J. Dropesky, G. C. Giesler, G. W. Butler, S. B. Kaufman, and E. P. Steinberg, Phys. Rev. C **30**, 1597 (1984).